

## ORIGINAL RESEARCH ARTICLE

# Protocol for a liver–bone organoid platform to study senescence-driven interorgan crosstalk

Jian Wang<sup>1†</sup>, Yingting Zhang<sup>2†</sup>, and Ming He<sup>2,3\*</sup>

<sup>1</sup>Department of Diagnostic Radiology, Yong Loo Lin School of Medicine, National University of Singapore, Singapore

<sup>2</sup>Key Laboratory of Cell Differentiation and Apoptosis of National Ministry of Education, Department of Pathophysiology, Shanghai Jiao Tong University School of Medicine, Shanghai, China

<sup>3</sup>Department of Orthopaedics, Xinhua Hospital, Shanghai Jiao Tong University School of Medicine, Shanghai, China

\*Corresponding authors: Ming He (heming@shsmu.edu.cn)

<sup>†</sup>These authors contributed equally to this work.

**Citation:** Wang J, Zhang Y, He M. Protocol for a liver–bone organoid platform to study senescence-driven interorgan crosstalk. *Organoid Res.* 2026;2(2):026170024. doi: 10.36922/OR026170024

**Received:** April 23, 2026

**Revised:** June 2, 2026

**Accepted:** June 9, 2026

**Published online:** June 26, 2026

**Copyright:** © 2026 Author(s). This is an Open-Access article distributed under the terms of the Creative Commons Attribution License, permitting distribution, and reproduction in any medium, which provided that the original work is properly cited.

**Publisher's Note:** AccScience Publishing remains neutral with regard to jurisdictional claims in published maps and institutional affiliations.

## Abstract

Liver–bone crosstalk is increasingly recognized as an important regulatory axis in aging-associated diseases, such as metabolic liver disease and osteoporosis. However, conventional two-dimensional co-culture systems and animal models do not adequately capture the multicellular architecture, extracellular matrix context, and bidirectional secretory communication that underlie interorgan senescence propagation. Here, we describe a protocol for constructing a senescent liver–bone organoid platform by integrating a bone matrix-inspired three-dimensional (3D) bioprinted bone organoid system with a mouse duct-derived liver organoid culture system, followed by engineered senescence induction and conditioned-medium exchange. In this protocol, bone marrow-derived mesenchymal stem cells are incorporated into a gelatin/alginate/hydroxyapatite hybrid bioink and printed into porous 3D constructs, whereas liver ductal structures are embedded in Matrigel and expanded into liver organoids before directed differentiation. Senescence is induced in both organoid types using doxorubicin, and systemic aging-related signals are modeled by treating organoids with serum from older mice. Bidirectional communication is then interrogated through reciprocal conditioned-medium transfer assays. This platform enables investigation of interorgan senescence propagation, liver–bone axis dysfunction, and candidate mediators such as 27-hydroxycholesterol in a physiologically relevant 3D setting.

**Keywords:** Liver–bone organoid; Liver–bone crosstalk; Senescence; 3D bioprinting

## 1. Introduction

Organoid technology has become an important experimental approach for reconstructing tissue cytoarchitecture and organ-specific function in a three-dimensional (3D) culture system that more closely resembles native physiology than conventional two-dimensional culture systems.<sup>1,2</sup> Among these models, bone organoids and liver organoids have each shown considerable value for studying lineage differentiation, matrix remodeling, and disease-associated phenotypes.<sup>3–6</sup> Bone organoid systems

based on bone marrow-derived mesenchymal stem cells (BMSCs), hydroxyapatite-containing hybrid bioinks, and digital light processing (DLP) bioprinting provide a robust platform for generating mineralization-capable bone-like structures<sup>7,8</sup>, whereas duct-derived mouse liver organoids are capable of expansion and differentiation into hepatocyte-like organoids under defined culture conditions.<sup>9</sup> Despite these advances, most currently available organoid models remain focused on single-organ biology and therefore do not adequately capture the biological complexity of communication between distinct tissues.<sup>10</sup> This limitation is

particularly relevant to the liver–bone axis, where growing evidence suggests that hepatic dysfunction and skeletal decline are mechanistically interconnected, especially in the process of aging.<sup>11</sup>

A significant challenge in modeling the liver–bone axis is the establishment of senescent organoid systems that are both biologically informative and experimentally reproducible.<sup>11</sup> In principle, organoids derived directly from aged tissues might be expected to provide the most physiologically relevant platform.<sup>12</sup> However, the liver–bone senescence study showed that this strategy was not sufficient to reliably generate both components of the model. Aged BMSCs displayed limited proliferative capacity and poor performance in the 3D hydrogel culture system, which compromised stable bone organoid formation, whereas organoids obtained from aged liver ductal structures failed to spontaneously develop a robust senescent phenotype.<sup>13</sup> These findings indicate that tissue age alone does not necessarily translate into a consistent organoid-level aging state *in vitro*.<sup>14</sup> For this reason, doxorubicin (DOX)-based induction was adopted as a controllable method for generating senescent bone and liver organoids.<sup>15</sup> Under these conditions, both organoid systems reproduced key aging-associated features, including reduced mineralization in bone organoids, increased senescence-associated  $\beta$ -galactosidase (SA- $\beta$ -gal) and cyclin-dependent kinase inhibitor 1A (p21) expression, phosphorylated histone H2AX ( $\gamma$ -H2AX) elevation under selected conditions, and lipid accumulation in liver organoids.<sup>16,17</sup>

On this basis, the present protocol is intended not merely to establish bone and liver organoids as independent culture systems, but to integrate them into a dual-organoid platform for investigating senescence-driven interorgan crosstalk. This workflow is adapted from the experimental strategy reported in Zhang *et al.*<sup>15</sup>, in which engineered senescent liver and bone organoid models were established to dissect bidirectional aging-associated communication between the two tissues. While our previous work demonstrated the biological relevance of liver–bone organoid crosstalk, the present protocol provides a standardized, step-by-step methodology that improves scalability and accessibility. By combining engineered bone organoid fabrication with liver organoid derivation and differentiation, and subsequently applying senescence induction, serum stimulation, and reciprocal conditioned-medium exchange, the workflow enables systematic interrogation of how aging-associated signals are transmitted between the two tissues (Figure 1). The resulting model provides a tractable framework for examining tissue-autonomous senescence and investigating the transmission of pro-senescent signals along the liver–bone axis, thereby offering a useful experimental system for mechanistic studies of multi-organ aging.

## 2. Development of liver–bone organoid cultures

The development of this protocol draws from two experimentally mature systems. The first is the hydroxyapatite hybrid bioink-based 3D bioprinted bone organoid method, in which BMSCs are embedded in a photocurable gelatin/alginate/hydroxyapatite matrix to generate porous mineralization-competent constructs. The second is the mouse liver organoid derivation method based on isolation of ductal structures, Matrigel embedding, expansion under niche-factor-containing medium, and subsequent differentiation into hepatocyte-like organoids.

To enable interorgan aging studies, this protocol adapts both systems into a unified workflow. Bone organoids are first matured under osteogenic induction conditions, while liver organoids are expanded and differentiated. Senescence is then induced in each organoid type using 0.5  $\mu$ M DOX. The resulting senescent organoids are used in three experimental branches: (i) direct phenotyping, (ii) treatment with young or aged serum, and (iii) reciprocal conditioned-medium transfer. This design allows investigation of both tissue-autonomous aging and non-cell-autonomous propagation of senescence signals.

## 3. Applications of the method and future possibilities

This protocol can be used in several settings. First, it enables mechanistic studies of the liver–bone axis under aging-related conditions by providing a controllable system in which each organoid can be independently manipulated and then tested for effects on the counterpart tissue. Second, it provides a platform for evaluating candidate mediators of interorgan communication. In the reference study, proteomic and functional analyses highlighted sterol metabolism dysregulation and identified 27-hydroxycholesterol as a liver-derived factor capable of inducing bone organoid senescence and impairing mineralization. This protocol can be adapted to test such metabolites, cytokines, extracellular vesicles, or secreted proteins. Third, it can be used for intervention studies, including testing whether pharmacological inhibitors, gene perturbations, or medium modifications disrupt senescence propagation between organoids. Finally, the protocol can serve as a foundation for future humanized or disease-specific versions, including platforms incorporating patient-derived organoids, additional stromal or immune components, vascularized systems, or organ-on-chip fluidic coupling. It should be noted that this model does not include immune cells, vasculature, or stromal components, which are known to modulate senescence-associated secretory phenotype (SASP) signaling and may influence interorgan crosstalk *in vivo*. Future integration of these elements will be important for full physiological recapitulation.

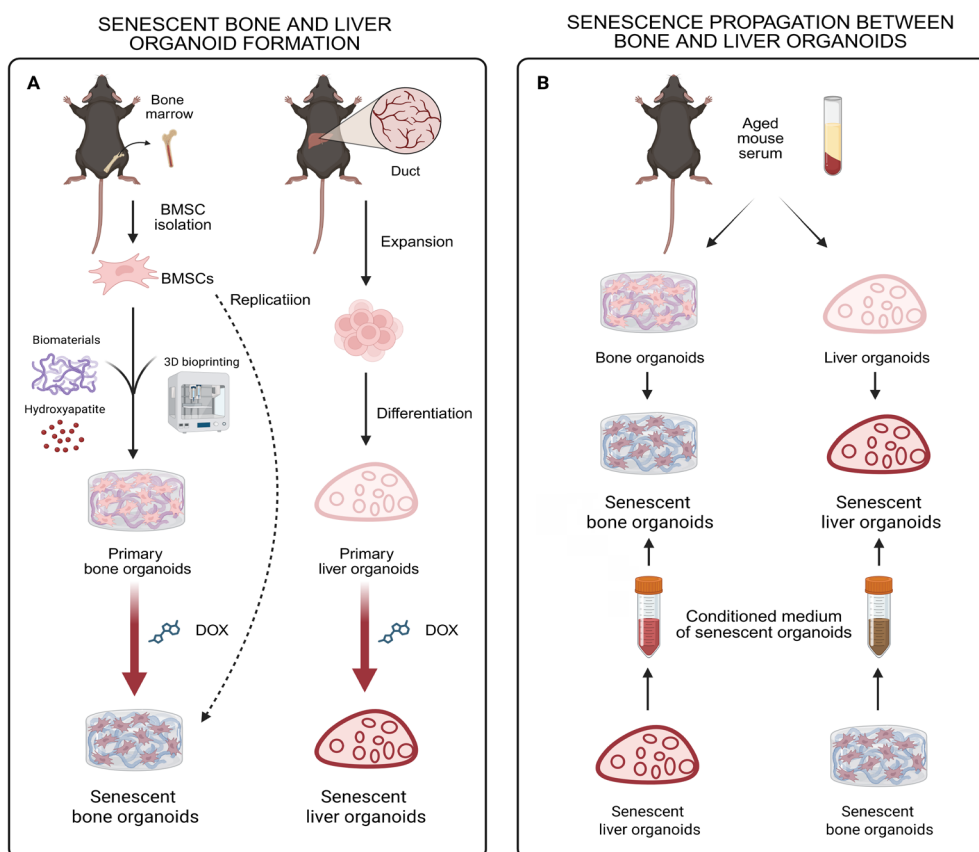


**Figure 1.** Schematic overview of the experimental protocol. (A) Formation of senescent mouse bone and liver organoids. (B) Evaluation of systemic senescence propagation between bone and liver.

Abbreviations: BMSC: Bone marrow-derived stem cell; DOX: Doxorubicin.

## 4. Experimental design

The experimental design comprises six sequential, interrelated procedures. Procedure 1 focuses on the preparation of the hydroxyapatite hybrid bioink and the isolation and propagation of BMSCs, thereby establishing the material and cellular basis for bone organoid fabrication. Procedure 2 involves the formation of bone organoids based on a DLP-based bioprinting strategy, followed by osteogenic induction to promote structural and functional maturation. In parallel, Procedure 3 involves the derivation of mouse liver organoids, including tissue isolation, expansion, passaging, and differentiation. Once both organoid systems reach a stable and mature state, Procedure 4 introduces DOX-induced senescence in bone and liver organoids to generate an experimental platform for modeling age-related interorgan interactions. Building on this foundation, Procedure 5 assesses systemic and paracrine modes of communication through treatment with serum from young or aged mice, as well as reciprocal

conditioned-medium exchange between the two organoid types. Finally, Procedure 6 encompasses the phenotypic characterization of both systems, with particular emphasis on senescence, mineralization, DNA damage, and lipid accumulation. Taken together, this workflow is designed as a stepwise platform that progresses from the independent establishment and maturation of each organoid system to the induction of aging-related perturbations, followed by interorgan communication assays and, ultimately, phenotypic and mechanistic interrogation of liver–bone crosstalk.

The following reagents and equipment are required for this protocol:

### (a) Reagents

Gelatin (cat. no. L434330, Aladdin, China); sodium alginate (cat. no. A434496, Aladdin, China); hydroxyapatite (cat. no. H106378, Aladdin, China); methacrylic anhydride (cat. no. 276685, Sigma-Aldrich, United States of America [USA]);

calcium chloride ( $\text{CaCl}_2$ ; cat. no. C598678, Aladdin, China); disodium hydrogen phosphate ( $\text{Na}_2\text{HPO}_4$ ; cat. no. D433613, Aladdin, China); sodium hydroxide ( $\text{NaOH}$ ; cat. no. S163080, Aladdin, China); anhydrous ethanol (cat. no. E7023, Sigma-Aldrich, USA); phosphate-buffered saline (PBS; cat. no. G4202, Servicebio, China); Dulbecco's modified Eagle medium (DMEM; cat. no. 11995065, Thermo Scientific, USA); type I collagenase (cat. no. SCR103, Sigma-Aldrich); fetal bovine serum (FBS; cat. no. 12103C, Sigma-Aldrich, USA); P/S (cat. no. P4333, Sigma-Aldrich); trypsin-EDTA (cat. no. 25200072, Thermo Scientific, USA); lithium phenyl-2,4,6-trimethylbenzoylphosphinate (LAP; cat. no. L157759, Aladdin, China); light absorber (cat. no. EFL-UVAW-001, EFL, China);  $\alpha$ -MEM (cat. no. 12571063, Thermo Scientific, USA);  $\beta$ -glycerophosphate (cat. no. D301908, Aladdin, China); ascorbic acid (cat. no. A103534, Aladdin, China); dexamethasone (cat. no. D137736, Aladdin, China); BALB/c nude mice (cat. no. C000103, Cavens, China); isoflurane (cat. no. 792632, Sigma-Aldrich, USA); Matrigel (cat. no. 356231, Corning, USA); Advanced Dulbecco's modified Eagle medium/nutrient mixture F-12 (Advanced DMEM/F12; cat. no. 12634010, Thermo Scientific, USA); B27 Supplement (cat. no. 17504044, Thermo Scientific, USA); N-2 Supplement (cat. no. 17502048, Thermo Scientific, USA); N-acetylcysteine (cat. no. A9165, Sigma-Aldrich, USA); R-spondin 1 conditioned medium (cat. no. 3474-RS, R&D Systems, USA); nicotinamide (cat. no. N0636, Sigma-Aldrich, USA); leu15-gastrin I (cat. no. G9145, Sigma-Aldrich, USA); epidermal growth factor (EGF; cat. no. AF-100-15, PeproTech, USA); fibroblast growth factor 10 (FGF10; cat. no. 100-26, PeproTech, USA); hepatocyte growth factor (cat. no. 100-39, PeproTech, USA); Y-27632 (ROCK inhibitor; cat. no. S1049, Selleck, USA); A83-01 (TGF- $\beta$  inhibitor; cat. no. S7692, Selleck, USA); DAPT (Notch inhibitor; cat. no. S2215, Selleck, USA); type IV collagenase (cat. no. 17104019, Thermo Scientific, USA); dispase II (cat. no. D4693, Sigma-Aldrich, USA); TrypLE Express Enzyme (cat. no. 12605010, Thermo Scientific, USA); BODIPY 493/503 (lipid stain; cat. no. D3922, Thermo Scientific, USA); DOX (cat. no. D1515, Sigma-Aldrich, USA); SA- $\beta$ -gal staining kit (cat. no. 9860, Cell Signaling Technology, USA); DAPI (cat. no. D1306, Thermo Scientific, USA); hematoxylin and eosin (H & E) staining kit (cat. no. G1005-100ML, Servicebio, China); Masson's trichrome staining kit (cat. no. G1006-100ML, Servicebio, China); Alizarin Red S solution (cat. no. G1038-100ML, Servicebio, China).

(b) Equipment/consumables/software

Magnetic stirrer (model no. TS-14SG, Lab Companion, South Korea); sterile 50 mL centrifuge tubes (cat. no. 602001, NEST, China); sterile 15 mL centrifuge tubes (cat. no. 601001, NEST, China); freeze dryer (FreeZone, Labconco, USA); 70  $\mu\text{m}$  cell strainer (cat. no. 258368, NEST, China); biosafety cabinet (model no. HFsafe-

1200LC, Heal Force, China); centrifuge (cat. no. 75007221, SL8R, Thermo Scientific, USA); cell culture incubator (cat. no. MCO-19AICUV-PE, Panasonic, Japan); 100 mm culture dishes (cat. no. 704004, NEST, China); light microscope (Eclipse TS100, Nikon, Japan); pipettes (cat. nos. 3123000039, 3123000055, and 3123000268, Eppendorf Research, Germany); 3D Studio Max software (Autodesk, USA); water bath (model no. WB-1-30, TATUNG, Taiwan); cell counter (model no. IC1000, Countstar, China); cell counting slides (cat. no. CO010101, Countstar, China); DLP printer (EFL-BP-8601 Pro, EFL, China); 0.22  $\mu\text{m}$  filters (cat. no. 331011, NEST, China); six-well plates (cat. no. 703001, NEST, China); isoflurane vaporizer (V60, Mindray, China); anesthesia machine (model no. F700, EZ Vet, China); sterile scalpel (RWD, China); sterile blunt forceps (RWD, China); and sterile surgical thread (RWD, China); 48-well cell culture plate (cat. no. 701201, NEST, China); 1.5 mL microcentrifuge tube (cat. no. MCT-150-C, Axygen, USA); 100  $\mu\text{m}$  cell strainer (cat. no. 350100, NEST, China); stereomicroscope (SMZ745, Nikon, Japan); confocal laser scanning microscope (LSM880, Zeiss, Germany).

#### 4.1. Procedure 1: Preparation of hydroxyapatite hybrid bioink and BMSC culture

##### 4.1.1. Synthesis of bioinspired bone matrix hydrogel

The hydroxyapatite hybrid hydrogel serves as the bone matrix-mimicking scaffold for BMSC-based bone organoid fabrication. Its composition and preparation are adapted from the bone organoid engineering protocol and are also consistent with the matrix system used in the liver–bone senescence study.

- Add 10 g of gelatin to 50 mL of deionized water in a 100 mL beaker. Stir at 50 °C and approximately 300 rpm until a clear, homogeneous 20 wt% solution is obtained.
- In a separate beaker, dissolve 0.5 g sodium alginate in 42 mL deionized water under stirring at ambient temperature for 4–6 h until a clear solution is obtained.
- Add 4 mL of 1 M  $\text{CaCl}_2$  and 4 mL of 0.6 M  $\text{Na}_2\text{HPO}_4$  gradually at approximately 50  $\mu\text{L}/\text{min}$ . Titrate the pH to 8–10 with 3 M  $\text{NaOH}$ , and continue stirring.
- Preheat both solutions to 50 °C, combine them, and stir thoroughly. Add 4 mL methacrylic anhydride gradually while maintaining the pH at 8–10. Continue the reaction at 50 °C for 3 h.
- Dilute with warm deionized water to stop the reaction and transfer the mixture into dialysis tubing with an approximate molecular weight cutoff of 13,000 Da. Dialyze the sample extensively against a large volume of deionized water for seven days, with water replaced twice per day.
- After dialysis, freeze the solution and subject it to freeze-drying to obtain the solid hydrogel material.



Store the dried product in a moisture-protected container until use.

The resulting material corresponds to a gelatin methacrylate (GelMA)/alginate methacrylate/hydroxyapatite-type hydrogel suitable for photocurable bone organoid bioprinting. In the liver–bone senescence study, this material was described as a bionic hydrogel with increased compressive performance relative to GelMA alone and was used to support the formation of bone organoids displaying age-related mineralization phenotypes.

#### 4.1.2. Isolation and culture of BMSCs

- Prepare a sterile operating field and sterilize all dissection tools. Use euthanized rodents in accordance with institutional animal ethics guidelines.
- Expose femurs and tibiae, remove the surrounding muscle carefully, and place the bones into cold sterile PBS.
- Remove the bone ends to expose the marrow cavity. Flush the marrow cavity with sterile PBS or culture medium and collect the outflow into a collection tube until the shafts appear pale. Disperse clumps by gentle pipetting.
- If desired for improved yield, incubate the marrow suspension with 0.1% type I collagenase at 37 °C for 30 min and filter through a 70- $\mu$ m cell filter.
- Collect cells by centrifugation at 300 $\times$ g for 5 min with the supernatant removed, then resuspend the cell pellet in growth medium. The bone protocol uses DMEM + 10% FBS + 1% penicillin–streptomycin (P/S), whereas the liver–bone senescence study used  $\alpha$ -MEM + 10% FBS + 1% P/S for BMSC culture. For consistency with the dual-organoid platform,  $\alpha$ -MEM-based culture is recommended.
- Plate cells and culture at 37 °C, 5% CO<sub>2</sub> for 24–48 h, then wash away non-adherent cells using PBS.
- Replace the culture medium every 2–3 days. Passage cells with trypsin-based detachment upon reaching 80–90% confluence. For organoid fabrication, early-passage BMSCs are preferred unless replicative senescence is specifically intended.

### 4.2. Procedure 2: Construction and maturation of bone organoids

#### 4.2.1. Preparation of bioink

- Solubilize LAP in  $\alpha$ -MEM with serum and antibiotics to obtain a 0.25 wt% solution.
- Add the light absorber to obtain a 0.5 wt% solution.
- Add the freeze-dried hydrogel powder to obtain a 10 wt% hydrogel solution. Maintain at 37 °C.
- Suspend BMSCs in this hydrogel to achieve a final density of  $1.0 \times 10^6$  cells/mL with all steps performed under light-protected conditions.

#### 4.2.2. 3D model design and digital light processing bioprinting

- Design a cylindrical scaffold using 3D modeling software. The bone protocol used a structure with a 7 mm diameter, a 2 mm thickness, and 21 evenly distributed square holes to facilitate the exchange of nutrients and soluble factors.
- Print the constructs using a DLP printer. Recommended parameters include a light intensity of 14 mW/cm<sup>2</sup> with an exposure time of 12 s for each layer. Print two base layers using a slightly prolonged exposure time of 14 s to ensure structural stability. Control the penetration depth at 50  $\mu$ m to maintain printing precision, and maintain the temperature of the printing chamber or platform at 37 °C throughout the process to preserve the rheological properties and printability of the bioink.
- Transfer the printed constructs into sterile PBS at 37 °C and rinse three times.

#### 4.2.3. Initial post-printing culture

Culture the printed bone organoids in  $\alpha$ -MEM + 10% FBS + 1% P/S for 3 days to allow recovery and stabilization.

#### 4.2.4. Osteogenic maturation

Replace the recovery medium with the osteogenic induction medium, which consists of a basal medium, either DMEM or  $\alpha$ -MEM as determined by laboratory standardization, supplemented with 10% FBS and 1% P/S. To promote osteogenic differentiation and matrix mineralization, enrich the medium with 10 mM  $\beta$ -glycerophosphate, 50  $\mu$ g/mL ascorbic acid, and 100 nM dexamethasone.

For the liver–bone senescence platform, maintain bone organoids under osteogenic induction for three weeks before senescence induction and conditioned-medium collection. This maturation period is recommended as the standard timeline for dual-organoid experiments.

### 4.3. Procedure 3: Derivation, expansion, and differentiation of liver organoids

#### 4.3.1. Derivation of liver organoids from mouse ductal structures

This step is adapted from the mouse liver organoid derivation workflow used in the liver–bone senescence study and is based on the established Broutier/Huch-type adult liver organoid method.<sup>18</sup>

- Excise the mouse liver and mince it into fragments of approximately 0.5 mm<sup>3</sup>.
- Transfer the fragments into the wash medium composed of DMEM + 1% P/S + 1% FBS and wash twice with repeated pipetting and settling.
- Digest the tissue in filter-sterilized digestion buffer

(wash medium supplemented with 0.125 mg/mL collagenase and Dispase II) and incubate at 37 °C for 1 h under continuous shaking. Meanwhile, check for the release of ductal structures periodically.

- (d) Collect the released structures, centrifuge at 300× g for 5 min, wash twice, and filter through a sieve with a mesh size of 100 μm. Retain the ductal cholangiocytic structures.
- (e) Resuspend the collected ductal structures in 200 μL Matrigel, dispense as 30 μL droplets in a 48-well plate, and allow the droplets to solidify for 5 min at 37 °C.
- (f) After solidification, overlay the Matrigel droplets with liver organoid expansion/isolation medium consisting of Advanced DMEM/F12 supplemented with 1% P/S, 2% B27, 1% N2, 1 mM N-acetylcysteine, 5% R-spondin1 conditioned medium, 10 mM nicotinamide, 10 nM Leu15-gastrin I, 50 ng/mL EGF, 100 ng/mL FGF10, and 50 ng/mL hepatocyte growth factor, together with an additional 30% L-WRN conditioned medium (containing Wnt3a, R-spondin 3, and Noggin) and 10 μM Y-27632 (a ROCK inhibitor).
- (g) Maintain cultures at 37 °C, 5% CO<sub>2</sub>, replacing the medium every 3–5 days.

#### 4.3.2. Passaging of liver organoids

- (a) Aspirate the medium.
- (b) Add 300 μL TrypLE and pipette approximately 10 times to dissociate the organoids.
- (c) Incubate for 4 min at ambient temperature.
- (d) Neutralize with twice the volume of DMEM/F12 containing 10% FBS.
- (e) Centrifuge at 500×g for 5 min.
- (f) Suspend the pellet in Matrigel and re-plate at approximately 1:4 split ratio as 30 μL droplets.
- (g) Overlay with fresh expansion medium and continue culture at 37 °C, 5% CO<sub>2</sub>.

#### 4.3.3. Differentiation of liver organoids

To obtain a more hepatocyte-like differentiated state suitable for senescence and metabolic assays:

- (a) Replace the isolation medium with expansion medium and culture for 3 days.
- (b) Transfer the cultures to a differentiation medium based on Advanced DMEM/F12 and supplemented with 1% P/S, 2% B27, 1 mM N-acetylcysteine, 10 nM Leu15-gastrin I, 50 ng/mL EGF, 100 ng/mL FGF10, 50 nM A83-01, and 10 μM DAPT. Culture the organoids for 9 days, with daily medium replacement to ensure stable exposure to differentiation cues and to support progressive maturation toward a more differentiated hepatic state.
- (c) For terminal maturation, add 3 μM dexamethasone to

the differentiation medium and incubate the mixture for an additional three days.

Differentiated liver organoids are then ready for senescence induction, serum treatment, or conditioned-medium experiments.

### 4.4. Procedure 4: Senescence induction in liver and bone organoids

#### 4.4.1. Doxorubicin induction of bone organoid senescence

The liver–bone senescence study optimized doxorubicin as a senescence inducer and selected 0.5 μM as an effective concentration that induced robust senescence while preserving acceptable viability.

- (a) Culture mature bone organoids under osteogenic induction for three weeks.
- (b) Add 0.5 μM DOX to the culture medium.
- (c) Incubate for either 3 days or 6 days.
- (d) For stronger senescence phenotypes, including more pronounced impairment of mineralization, the 6-day treatment is recommended.

Bone organoids treated under these conditions are expected to show increased SA-β-gal, p21, and γ-H2AX, along with reduced bone mineral density (BMD), bone volume/total volume (BV/TV), and trabecular thickness (Tb.Th).

#### 4.4.2. Doxorubicin induction of liver organoid senescence

- (a) Use liver organoids after completion of the differentiation program.
- (b) Add 0.5 μM DOX to the organoid culture medium.
- (c) Incubate for 3 days or 6 days.
- (d) The six-day condition is expected to induce stronger DNA damage and steatotic phenotypes, with higher p21, SA-β-gal, γ-H2AX, and boron-dipyrromethene (BODIPY) staining.

This engineered senescence method is preferred over direct establishment from aged ductal tissues because aged-duct-derived liver organoids did not reproducibly display robust spontaneous senescent phenotypes in the study.

#### 4.4.3. Optional replicative senescence model for bone organoids

If a long-term passage model is desired, BMSCs can also be expanded to late passage, such as P23, to generate replicatively senescent bone organoids. However, for dual-organoid crosstalk experiments, the DOX-induced model is generally more practical and standardized.

#### **4.5. Procedure 5: Serum treatment and interorgan conditioned-medium exchange**

##### **4.5.1. Young and aged mouse serum treatment**

This procedure models the contribution of circulating systemic aging factors to organoid senescence.

- (a) Collect serum from young and aged mice, such as 4- and 14-month-old mice.
- (b) After liver organoid differentiation and bone organoid maturation, supplement the culture medium with 10% mouse serum.
- (c) Maintain cultures at 37 °C, 5% CO<sub>2</sub>. Renew the medium every 2 days and continue for 1 week.

Aged serum is expected to induce SA- $\beta$ -gal in liver organoids and promote senescence-marker elevation plus mineralization impairment in bone organoids.

##### **4.5.2. Collection of conditioned medium from senescent bone organoids**

- (a) Generate senescent bone organoids by treating mature bone organoids with 0.5  $\mu$ M DOX for six days.
- (b) Wash the organoids using DOX-free culture medium three times to remove residual inducer.
- (c) Re-culture the organoids in freshly prepared osteogenic induction medium for 24 h.
- (d) Collect the supernatant at the end of this period as senescent bone organoid conditioned medium.

##### **4.5.3. Collection of conditioned medium from senescent liver organoids**

- (a) Generate senescent liver organoids by treating differentiated liver organoids with 0.5  $\mu$ M DOX for six days.
- (b) Wash the organoids using DOX-free culture medium three times.
- (c) Re-culture in fresh medium for 24 h.
- (d) Collect the supernatant as senescent liver organoid conditioned medium. The study notes that comparable conditioned media from control organoids should also be collected as matched controls.

##### **4.5.4. Reciprocal conditioned-medium transfer assay**

- (a) Treat differentiated liver organoids with control or senescent bone organoid conditioned medium.
- (b) In parallel, expose mature bone organoids to conditioned medium derived from either control or senescent liver organoids in order to evaluate liver-to-bone senescence propagation, and perform the reciprocal bone-to-liver communication assay by treating liver organoids with conditioned medium collected from control or senescence-induced bone organoids. Accordingly, the experimental design incorporated four comparison groups: control liver

organoids receiving conditioned medium from control bone organoids, liver organoids receiving conditioned medium from senescent bone organoids, bone organoids receiving conditioned medium from control liver organoids, and bone organoids receiving conditioned medium from senescent liver organoids. This bidirectional framework allows systematic assessment of both baseline interorgan signaling and senescence-associated paracrine crosstalk between the two organoid systems.

This assay is used to quantify bidirectional senescence propagation and to identify liver-to-bone versus bone-to-liver effects.

#### **4.6. Procedure 6: Characterization and phenotypic analysis of liver–bone organoids**

##### **4.6.1. Immunofluorescence staining**

Embed bone organoids in OCT medium and cut frozen sections at 10  $\mu$ m, while liver organoids can be stained whole-mount or after embedding, depending on laboratory preference.

- (a) Fix the sections or organoids in 4% paraformaldehyde for 5 min at room temperature.
- (b) Permeabilize with 0.1% Triton X-100 for 30 min at 4 °C.
- (c) Block with 3% bovine serum albumin for 1 h.
- (d) Incubate the samples overnight at 4 °C with primary antibodies directed against senescence- and DNA damage-associated markers, including anti-p21 and anti- $\gamma$ -H2AX, each used at a dilution of 1:200, to enable subsequent detection of cell-cycle arrest and DNA damage responses within the organoid tissues.
- (e) After washing, incubate with Alexa Fluor-conjugated secondary antibodies and DAPI for 1 h at room temperature.
- (f) For fluorescent SA- $\beta$ -gal detection, incubate with the  $\beta$ -gal probe (for example, XZ1208, 10  $\mu$ M) overnight before imaging.

This staining panel is suitable for evaluating senescence burden and DNA damage in both liver and bone organoids.

##### **4.6.2. Histological analysis of bone organoids**

For bone organoids:

- (a) Fix in 4% PFA for 24 h.
- (b) Dehydrate, paraffin-embed, and section at 5  $\mu$ m.
- (c) Subsequently, process the samples for H & E staining for general histomorphological evaluation, Masson's trichrome staining to assess collagen deposition and extracellular matrix organization, and Alizarin Red S (ARS) staining to examine calcium deposition and the degree of matrix mineralization.

In the bone organoid protocol article, additional analyses, such as alkaline phosphatase (ALP), tartrate-resistant acid phosphatase, Oil Red O, toluidine blue, osteopontin, and osteocalcin, were also used to assess multicellular differentiation and matrix maturation. These may be incorporated if a broader characterization of bone identity is desired.

#### **4.6.3. SA- $\beta$ -gal histochemistry**

Cells or sections may also be fixed with  $\beta$ -gal staining fixative and incubated overnight at 37 °C under CO<sub>2</sub>-free conditions in X-gal developing solution. This is useful as an orthogonal validation method for senescence in monolayer BMSCs or alpha mouse liver 12 (AML12) cells and may also be adapted to organoid-derived sections.

#### **4.6.4. Lipid accumulation analysis in liver organoids**

In order to assess metabolic dysfunction in senescent liver organoids, perform BODIPY (lipid stain) staining. DOX-treated liver organoids are expected to show increased lipid droplet accumulation relative to controls.

#### **4.6.5. Western blot analysis**

Cell lysates or organoid lysates can be analyzed by sodium dodecyl sulfate-polyacrylamide gel electrophoresis and immunoblotting for senescence markers: p21, p16, and p53. These markers were used in the reference study to validate senescence induction in AML12 hepatocytes and related systems.

#### **4.6.6. Micro-computed tomography evaluation of bone organoids**

Assess bone organoids using micro-computed tomography (CT) using acquisition settings adapted from the liver–bone senescence study, including a tube voltage of 65 kV, a current of 80  $\mu$ A, an aluminum filter, and an image resolution of 13.8  $\mu$ m per pixel. Perform quantitative analysis of the reconstructed datasets to determine key structural and mineralization-related parameters, including BMD, BV/TV, Tb.Th, trabecular number, and trabecular separation.<sup>15</sup> These data are particularly important for evaluating the effect of senescence, aged serum, conditioned medium, or 27-hydroxycholesterol on osteogenic performance.

#### **4.6.7. Optional metabolite perturbation using 27-hydroxycholesterol**

If the protocol is extended toward mediator validation, bone organoids may be treated with 27-hydroxycholesterol for 6 days to model liver-derived pro-senescent signaling. The study identified 27-hydroxycholesterol as capable of inducing bone organoid senescence and impairing mineralization, with synergy observed when combined with DOX.

## **5. Validation of the protocol**

### **5.1. Validation of the senescent bone organoid protocol**

In bone organoid experiments, DOX was applied following three weeks of culture, with treatment durations of either 3 or 6 days (Figure 2A). H & E staining of bone organoids revealed that the bone organoids induced by DOX exhibited extensive vacuolization within the hydrogel matrix, disruption of fibrous extracellular matrix architecture, disorganized cellular alignment, and irregular patchy eosin staining patterns. Masson's trichrome staining revealed a significant reduction in red-stained mineralized structures in bone organoids following induction of senescence by DOX. ARS staining results showed that the calcium deposition in the DOX group was significantly less than in the control group (Figure 2B). DOX significantly compromised bone matrix mineralization (Figure 2C). Enhanced SA- $\beta$ -gal activity, p21 expression, and  $\gamma$ -H2AX levels in DOX-induced bone organoids demonstrated that the protocol could successfully trigger both the senescence cascade and the DNA damage signaling pathway (Figure 2D).

### **5.2. Validation of the senescent liver organoids protocol**

Following the generation of mouse liver organoids from mouse hepatobiliary tissue, DOX was also employed to induce senescence (Figure 3A–3B). SA- $\beta$ -gal activity and p21 expression increased significantly following DOX treatment for either 3 or 6 days. Notably,  $\gamma$ -H2AX immunostaining revealed that the 6-day DOX exposure caused more severe DNA damage than 3 days of treatment (Figure 3C). To functionally validate the structural and metabolic alterations associated with senescence in liver organoids, we examined key hallmarks of metabolic aging. DOX treatment led to a significant accumulation of lipid droplets, as visualized by BODIPY staining, confirming the presence of steatosis, a characteristic feature of aged or dysfunctional hepatocytes (Figure 3D). Collectively, these results demonstrate that this protocol recapitulates both canonical senescence markers and metabolic dysfunction, thereby extending the utility of DOX-based induction as a reliable multi-tissue senescence induction approach applicable to both bone and liver organoid systems.

### **5.3. Aged mouse serum-induced organoid senescence**

To investigate the systemic transmission of aging signals, serum collected from the mice aged 4 and 14 months was employed to treat both liver and bone organoids. The exposure to the serum from 14-month-old aged mice induced marked and tissuespecific senescence responses. In liver organoids, we observed a marked elevation of SA- $\beta$ -gal



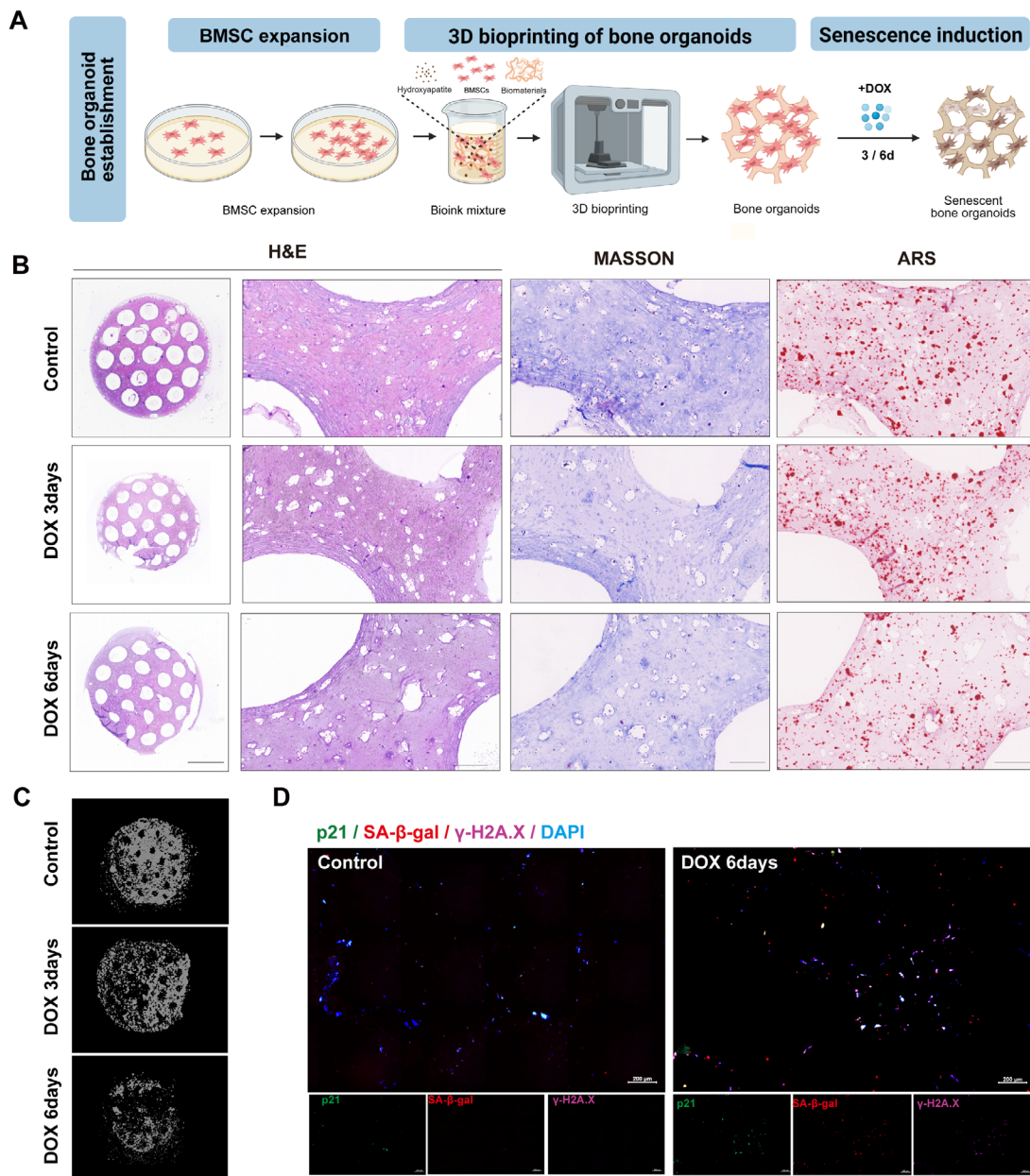


**Figure 2.** Dysfunction and characteristics of senescent bone organoids. (A) Procedural schematic for senescent bone organoids construction. Bone organoids were treated with 0.5  $\mu$ M DOX for 3 and 6 days. (B) H & E (left: scale bars: 2.5 mm; right: scale bars: 200  $\mu$ m), Masson (scale bars: 200  $\mu$ m), and ARS staining (scale bars: 200  $\mu$ m). (C) Representative micrographs of 3D mineralization. (D) Immunofluorescence staining of p21 (green), SA- $\beta$ -gal (red),  $\gamma$ -H2AX (purple), and DAPI (blue). Scale bars: 200  $\mu$ m.

Abbreviations: ARS: Alizarin Red S staining; BMSCs: Bone marrow-derived stem cells; DOX: Doxorubicin; H & E: Hematoxylin and eosin.

(Figure 4A). In bone organoids, the significant upregulation of SA- $\beta$ -gal, p21, and  $\gamma$ -H2AX was observed (Figure 4B). Beyond molecular markers, functional impairment was evident in the bone compartment. Micro-CT analysis revealed a reduction in mineralization; 14-month-old mice

serum treatment groups showed significantly lower mineral deposition, relative to control cultures supplemented with serum from young mice (Figure 4C). The aged mouse serum treatment-induced bone matrix degeneration was further supported by H & E, Masson, ARS, and ALP

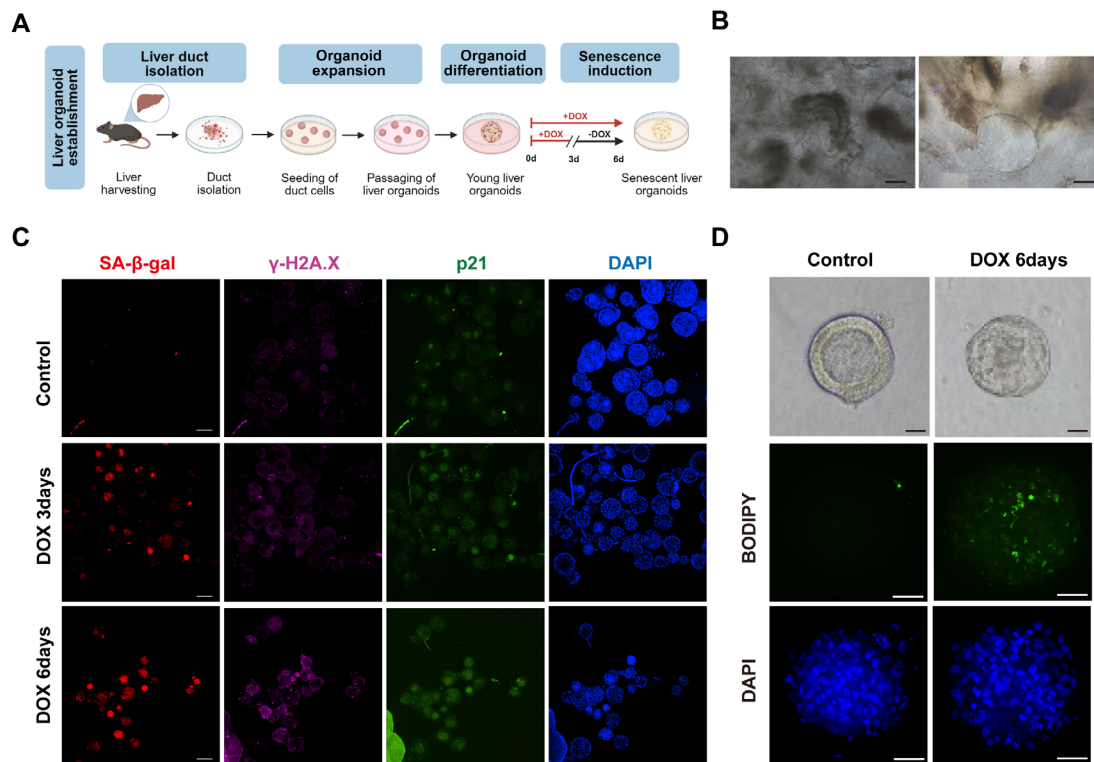


**Figure 3.** Dysfunction and characteristics of senescent liver organoids. (A) Procedural schematic for the construction of senescent liver organoids. (B) Bright-field images of the ducts isolated from the liver and lumen-containing organoid structures on day 2 after isolation in culture. Scale bars: left: 50  $\mu\text{m}$ ; right: 10  $\mu\text{m}$ . (C) Immunofluorescence staining of p21 (green), SA- $\beta$ -gal (red),  $\gamma$ -H2AX (purple), and DAPI (blue) in liver organoids treated with 0.5 $\mu\text{M}$  doxorubicin (DOX) for 3 and 6 days. Scale bars: 200  $\mu\text{m}$ . (D) Lipid deposition of liver organoids. Scale bars: 100  $\mu\text{m}$ .

staining (Figure 4D). Collectively, these findings provide direct evidence that circulating bloodborne factors from aged organisms are sufficient to induce cellnonautonomous senescence across distinct tissue types, underscoring the physiological relevance of developing a protocol to study inter-organoid interactions under senescent conditions.

#### 5.4. Interaction between senescent liver and bone organoids

To extend our observations on systemic aging signals, we next asked whether paracrine mechanisms were sufficient to drive cross-organ senescence interaction. Conditioned medium was therefore collected from donor liver or bone organoids following six days of DOX-induced senescence, after a 24-h washout period to remove residual drug. When applied to naïve recipient organoids, SA- $\beta$ -gal activity increased significantly in liver organoids treated with conditioned medium from senescent bone organoids (Figure 5A). Conversely, conditioned medium from senescent mouse liver organoids increased SA- $\beta$ -gal,

p21, and  $\gamma$ -H2AX signals and impaired bone organoid function (Figure 5B–5C). Supporting these quantitative findings, histomorphometric analysis further confirmed bone matrix degeneration (Figure 5D). Collectively, these results demonstrate the importance of establishing a senescent liver–bone organoid interaction protocol. This platform provides a practical *in vitro* model and effectively recapitulates systemic aging communication *in vivo*, confirming that liver and bone organoids bidirectionally transmit pro-aging signals.

#### 6. Limitations

Although the model can be used as a controllable experimental platform for studying senescence-driven liver–bone communication, the model has several important limitations, which should be taken into account when interpreting the research results. First, although the system captures the key aspects of parenchymal organoid behavior and interorgan signaling mediated by soluble factors, it cannot fully reproduce the cellular complexity of native

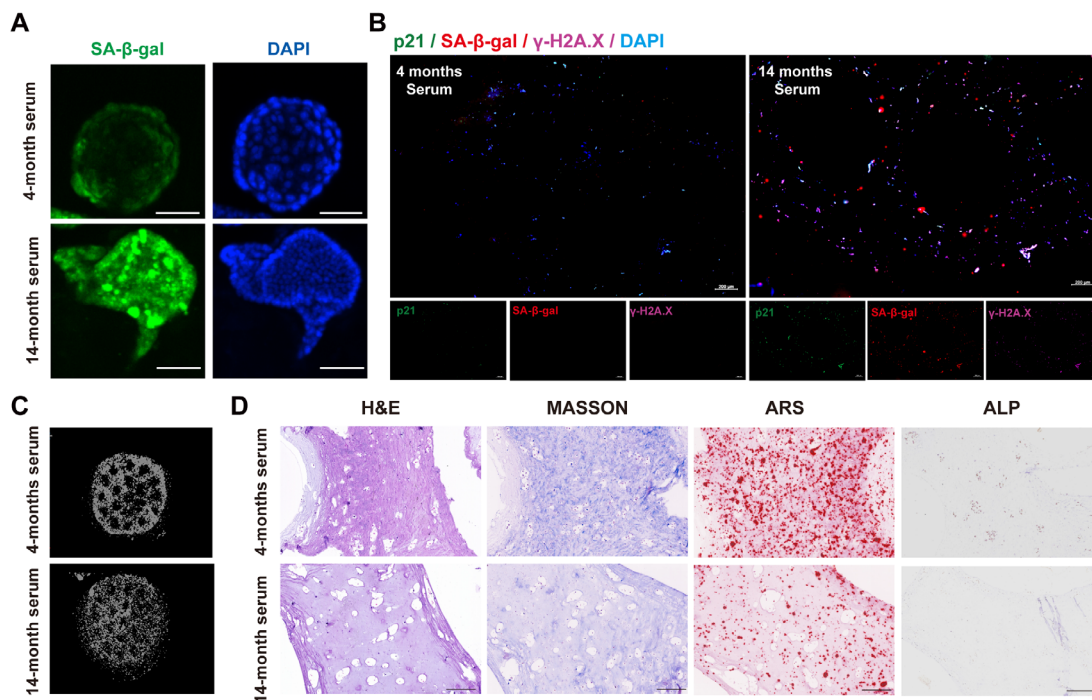


**Figure 4.** Aged serum-induced organoid senescence. Serum from the 4-month-old and 14-month-old mice was employed to treat both liver and bone organoids. (A) SA- $\beta$ -gal (green) in liver organoids. Scale bars: 100  $\mu$ m. (B) p21 (green), SA- $\beta$ -gal (red),  $\gamma$ -H2A.X (purple), and DAPI (blue) in bone organoids. Scale bars: 200  $\mu$ m. (C) Representative micro-computed tomography images of 3D mineralization. (D) H & E, Masson, ARS, and ALP staining of bone organoids. Scale bars: 200  $\mu$ m.

Abbreviations: ALP: Alkaline phosphatase; ARS: Alizarin Red S staining; H & E: Hematoxylin and eosin.

liver and bone tissues.<sup>19,20</sup> In particular, the current platform lacks several components that may affect the response of aging-related tissues *in vivo*, including vascular networks, immune cell populations, nerve inputs, and a broader bone marrow niche.<sup>21,22</sup> Especially for bone organoids, the lack of resorption chambers rich in osteoclasts and the vascular interface of physiological tissue means that the model mainly reflects the matrix generation and mineralization associated with osteoblasts, rather than the complete dynamic balance of bone turnover.<sup>23</sup> Similarly, although the liver organoid retains important epithelial features, it cannot fully reproduce the multicellular structure of the hepatic microenvironment, including Kupffer cells, hepatic stellate cells, endothelial cells, and their contributions to inflammation or fibrotic aging phenotype.<sup>24</sup>

The second limitation is related to the way of inducing aging. In this platform, aging is mainly introduced through DOX treatment, which provides a robust and repeatable method of producing age-like phenotypes during actual experiments. However, DOX-induced aging represents an engineered stress response, not a complete reappearance

of physiological aging.<sup>25,26</sup> Natural aging is caused by the cumulative interaction of genomic instability, epigenetic drift, mitochondrial dysfunction, altered nutrient sensing, chronic low-grade inflammation, extracellular matrix remodeling, and long-term systemic metabolic changes.<sup>27</sup> In contrast, DOX acts mainly through acute genotoxic stress and DNA damage, so it only simulates part of the aging process.<sup>26</sup> Although this method has successfully induced typical aging-related features, such as p21 upregulation, SA- $\beta$ -gal positivity, and DNA damage response, it should not be interpreted as equivalent to physiological aging *in vivo*.

Third, the platform relies on the conditioned-medium exchange strategy to simulate the communication between organs. This design is advantageous because it allows the controllable separation of paracrine signaling between two organoid systems, while avoiding the mixed effects of incompatible culture conditions.<sup>28</sup> However, it also simplifies the biology of the liver–bone axis. *In vivo*, liver–bone communication occurs in a more complex system environment composed of circulatory metabolites,



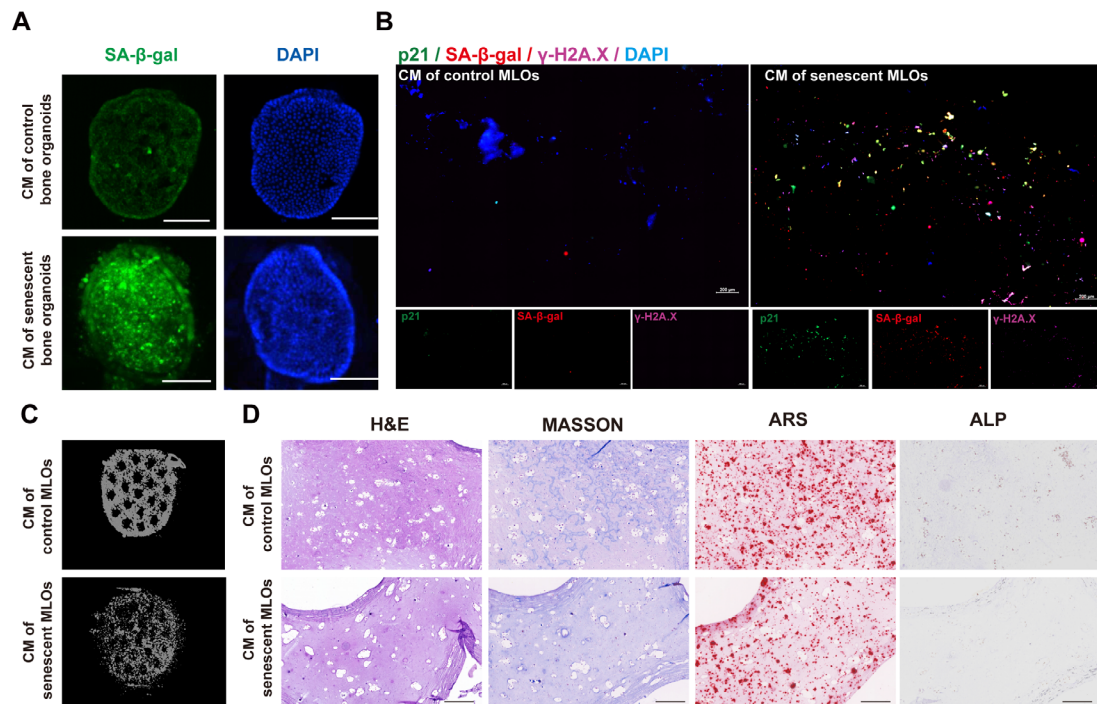


**Figure 5.** Validation of senescent liver–bone crosstalk based on the protocol. (A) SA-β-gal (green) in liver organoids following exposure to conditioned medium derived from senescent bone organoids. Scale bars: 100  $\mu$ m. CM derived from senescent liver organoids was added to bone organoid cultures. (B) Immunofluorescence staining of p21 (green), SA-β-gal (red),  $\gamma$ -H2AX (purple), and DAPI (blue). Scale bars: 200  $\mu$ m. (C) Representative micro-computed tomography images of 3D mineralization. (D) H & E, Masson, ARS, and ALP staining of bone organoids. Scale bars: 200  $\mu$ m. Abbreviations: ALP: Alkaline phosphatase; ARS: Alizarin Red S staining; CM: Conditioned medium; H & E: Hematoxylin and eosin; MLOs: Mouse liver organoids.

endocrine signals, extracellular vesicles, hemodynamic factors, and temporal feedback loops between multiple organs.<sup>29</sup> The current method only captures one aspect of interorgan communication, focusing on the influence of soluble factors derived from organoid-conditioned culture medium. Therefore, it may not fully reflect the complexity of cell-cell direct interaction, dynamic metabolic exchange, or system-level regulatory processes.<sup>30</sup>

Technically, while the conditioned-medium exchange method is convenient and avoids culture condition conflicts, it does not model the dynamic, continuous, bidirectional communication that occurs via the circulatory system *in vivo*. This approach captures only long-term accumulated secreted factors and loses critical information, including temporal dynamics of signal release, concentration gradients, and flow-mediated dilution effects. Future integration of microfluidic perfusion systems may help address these limitations. In addition, although we included extensive washing and a 24 h recovery period, trace amounts of residual DOX in conditioned medium cannot be completely ruled out. Future studies using DOXfree

senescence inducers would further validate the observed interorgan senescence propagation.

Another important limitation is that the bone module used in this protocol is adapted from a protocol originally designed to support the mature bone organoids *in vivo* after subcutaneous implantation.<sup>31</sup> However, in the current liver–bone interaction framework, the bone organoid system is reused as an *in vitro* platform mainly for maturation, aging induction, and conditional culture medium research. Although this adaptation is useful experimentally, it may reduce the degree to which the model reproduces the structural complexity, vascularization, and full maturity potential in the original *in vivo* implementation.<sup>32</sup> Meanwhile, the absence of immune and vascular components likely reduces the complexity of SASP-mediated signaling, as inflammatory cytokines and growth factors *in vivo* are often processed or amplified by these cells. Microfluidic co-culture systems or the incorporation of immune organoids could address this gap in future iterations. Therefore, in this improved



workflow, the absolute degree of mineralization and tissue organization may not fully match the source bone organoid system. In addition, the source study showed that it is not easy to derive organoids directly from aging primary cells. Aging BMSCs showed limited proliferation ability and poor performance in the 3D hydrogel environment, and the liver organoids originating from aging ductal progenitors did not show a strong enough aging phenotype.<sup>15</sup> These observations prove that it is reasonable to use engineered aging induction in this model, but they also highlight a broader limitation: the system has not yet fully captured the inherent heterogeneity and long-term biological history of natural aging tissue.<sup>33</sup> Therefore, although the model is very suitable for mechanism research and comparative disturbance experiments, it is still close to aging, rather than a direct reconstruction of the state of aging organisms.

Finally, mechanistic conclusions derived from the platform should be carefully interpreted. For example, determining that 27-hydroxycholesterol is a candidate mediator for liver–bone aging transmission is an important advantage of the system, but the dose-related inconsistency reported in different parts of the source study still needs to be further optimized and independently verified.<sup>34</sup> More broadly, before reaching an exact conclusion on causality or translational correlation, ideally, any mediator found in the model should be verified in a complementary system, including more complex organoid co-culture models, microphysiological platforms, and *in vivo* models.<sup>34–36</sup> Therefore, the future iteration of the platform will benefit from the inclusion of more matrix, immunity, vascular, and remodeling components, as well as the use of patient-sourced or disease-specific organoids, to improve physiological fidelity and better capture the complexity of age-related liver–bone pathology.

## 7. Conclusion

In conclusion, this liver–bone organoid platform provides a robust and reproducible approach for modeling interorgan communication *in vitro*. The system recapitulates key features of liver–bone crosstalk and offers a versatile experimental framework for studying age-related pathologies, elucidating their underlying molecular mechanisms, and assessing potential therapeutic interventions. With further optimization and the incorporation of greater biological complexity, this platform may serve as a powerful tool for both basic research and translational applications in regenerative medicine and age-related disease research.

## Acknowledgments

None.

## Funding

This study was funded by Noncommunicable Chronic Diseases-National Science and Technology Major Project (2024ZD0530900).

## Conflict of interest

Ming He serves as an Editorial Board Member of this journal, but was not in any way involved in the editorial and peer-review process conducted for this paper, directly or indirectly. The authors declare that they have no competing interests.

## Author contributions

*Conceptualization:* Ming He  
*Data curation:* Yingting Zhang  
*Formal analysis:* Yingting Zhang  
*Funding acquisition:* Ming He  
*Investigation:* Yingting Zhang  
*Project administration:* Ming He  
*Supervision:* Ming He  
*Writing—original draft:* Jian Wang, Yingting Zhang  
*Writing—review & editing:* Ming He

## Ethics approval and consent to participate

No new human participants, human tissue, or animal experiments were performed for the preparation of this protocol manuscript. However, implementation of the protocol involves animal-derived tissues or serum and should be conducted only after approval by the relevant institutional animal care and use committee.

## Consent for publication

Not applicable.

## Availability of data

All data supporting the findings of this protocol are available within the article and its supplementary information files. Additional data related to this protocol are available from the corresponding author upon reasonable request.

## References

1. Zhang J, Wu Y, Shen T, *et al*. Organoid research: new concepts and new technologies. *Burns Trauma*. 2026;14.  
doi: 10.1093/burnst/tkag015
2. Wang J, Xia Z, Su J. Organoid research breakthroughs in 2024: A review. *Organoid Res*. 2025;1(2):025040005.  
doi: 10.36922/or025040005
3. Shen Y, Benlabiod C, Watson E, *et al*. comBO: A combined human bone and lympho-myeloid bone marrow organoid

- for preclinical modeling of hematopoietic disorders. *Cell Stem Cell*. 2026;33(3):421-437.e7.  
doi: 10.1016/j.stem.2026.01.010
4. Hendriks D, Brouwers JF, Hamer K, *et al*. Engineered human hepatocyte organoids enable CRISPR-based target discovery and drug screening for steatosis. *Nat Biotechnol*. 2023;41(11):1567-1581.  
doi: 10.1038/s41587-023-01680-4
  5. Khan AO, Rodriguez-Romera A, Reyat JS, *et al*. Human Bone Marrow Organoids for Disease Modeling, Discovery, and Validation of Therapeutic Targets in Hematologic Malignancies. *Cancer Discov*. 2022;13(2):364-385.  
doi: 10.1158/2159-8290.cd-22-0199
  6. Tadokoro T, Murata S, Kato M, *et al*. Human iPSC–liver organoid transplantation reduces fibrosis through immunomodulation. *Sci Transl Med*. 2024;16(757).  
doi: 10.1126/scitranslmed.adg0338
  7. Wang J, Wu Y, Li G, *et al*. Engineering Large-Scale Self-Mineralizing Bone Organoids with Bone Matrix-Inspired Hydroxyapatite Hybrid Bioinks (Adv. Mater. 30/2024). *Adv Mater*. 2024;36(30).  
doi: 10.1002/adma.202470239
  8. Zhang P, Qin Q, Cao X, Xiang H, Feng D, Wusiman D, Li Y. Hydrogel microspheres for bone regeneration through regulation of the regenerative microenvironment. *Biomater Transl*. 2024;5(3):205-235.  
doi: 10.12336/biomatertransl.2024.03.002
  9. Prior N, Inacio P, Huch M. Liver organoids: from basic research to therapeutic applications. *Gut*. 2019;68(12):2228-2237.  
doi: 10.1136/gutjnl-2019-319256
  10. Rossi G, Manfrin A, Lutolf MP. Progress and potential in organoid research. *Nat Rev Genet*. 2018;19(11):671-687.  
doi: 10.1038/s41576-018-0051-9
  11. Tysoe O. Liver–bone crosstalk implicated in osteoporosis progression. *Nat Rev Endocrinol*. 2023;19(8):440-440.  
doi: 10.1038/s41574-023-00859-8
  12. Kim J, Koo BK, Knoblich JA. Human organoids: model systems for human biology and medicine. *Nat Rev Mol Cell Biol*. 2020;21(10):571-584.  
doi: 10.1038/s41580-020-0259-3
  13. Ambrosi TH, Scialdone A, Graja A, *et al*. Adipocyte Accumulation in the Bone Marrow during Obesity and Aging Impairs Stem Cell-Based Hematopoietic and Bone Regeneration. *Cell Stem Cell*. 2017;20(6):771-784.e6.  
doi: 10.1016/j.stem.2017.02.009
  14. Pitrez PR, Monteiro LM, Borgogno O, Nissan X, Mertens J, Ferreira L. Cellular reprogramming as a tool to model human aging in a dish. *Nat Commun*. 2024;15(1).  
doi: 10.1038/s41467-024-46004-5
  15. Zhang Y, Li Y, Wang F, *et al*. Liver-bone organoids reveal senescence-driven interorgan crosstalk. *Bioact Mater*. 2025;54:570-583.  
doi: 10.1016/j.bioactmat.2025.08.039
  16. Ogrodnik M, Miwa S, Tchkonja T, *et al*. Cellular senescence drives age-dependent hepatic steatosis. *Nat Commun*. 2017;8(1).  
doi: 10.1038/ncomms15691
  17. Wang J, Zhang Y, Wang S, Wang X, Jing Y, Su J. Bone aging and extracellular vesicles. *Sci Bull*. 2024;69(24):3978-3999.  
doi: 10.1016/j.scib.2024.10.013
  18. Broutier L, Andersson-Rolf A, Hindley CJ, *et al*. Culture and establishment of self-renewing human and mouse adult liver and pancreas 3D organoids and their genetic manipulation. *Nat Protoc*. 2016;11(9):1724-1743.  
doi: 10.1038/nprot.2016.097
  19. Sljukic A, Green Jenkinson J, Niksic A, Prior N, Huch M. Advances in liver and pancreas organoids: how far we have come and where we go next. *Nat Rev Gastroenterol Hepatol*. 2025;23(1):44-64.  
doi: 10.1038/s41575-025-01116-1
  20. Bai L, Zhou D, Li G, Liu J, Chen X, Su J. Engineering bone/cartilage organoids: strategy, progress, and application. *Bone Res*. 2024;12(1).  
doi: 10.1038/s41413-024-00376-y
  21. Hofer M, Lutolf MP. Engineering organoids. *Nat Rev Mater*. 2021;6(5):402-420.  
doi: 10.1038/s41578-021-00279-y
  22. McWilliam RH, Chang W, Liu Z, Wang J, Han F, Black RA, Wu J, Luo X, Li B, Shu W. Three-dimensional biofabrication of nanosecond laser micromachined nanofibre meshes for tissue engineered scaffolds. *Biomater Transl*. 2023;4(2):104-114.  
doi: 10.12336/biomatertransl.2023.02.005
  23. Wang J, Chen X, Li R, *et al*. Standardization and consensus in the development and application of bone organoids. *Theranostics*. 2025;15(2):682-706.  
doi: 10.7150/thno.105840
  24. Afonso MB, Marques V, van Mil SWC, Rodrigues CMP. Human liver organoids: From generation to applications. *Hepatology*. 2023;79(6):1432-1451.  
doi: 10.1097/hep.0000000000000343
  25. Ogrodnik M, Carlos Acosta J, Adams PD, *et al*. Guidelines for minimal information on cellular senescence experimentation *in vivo*. *Cell*. 2024;187(16):4150-4175.  
doi: 10.1016/j.cell.2024.05.059
  26. Linders AN, Dias IB, López Fernández T, Tocchetti CG,

- Bomer N, Van der Meer P. A review of the pathophysiological mechanisms of doxorubicin-induced cardiotoxicity and aging. *npj Aging*. 2024;10(1).  
doi: 10.1038/s41514-024-00135-7
27. López-Otín C, Blasco MA, Partridge L, Serrano M, Kroemer G. Hallmarks of aging: An expanding universe. *Cell*. 2023;186(2):243-278.  
doi: 10.1016/j.cell.2022.11.001
  28. Leung CM, de Haan P, Ronaldson-Bouchard K, *et al*. A guide to the organ-on-a-chip. *Nat Rev Methods Primers*. 2022;2(1).  
doi: 10.1038/s43586-022-00118-6
  29. Gough A, Soto-Gutierrez A, Verneti L, Ebrahimkhani MR, Stern AM, Taylor DL. Human biomimetic liver microphysiology systems in drug development and precision medicine. *Nat Rev Gastroenterol Hepatol*. 2020;18(4):252-268.  
doi: 10.1038/s41575-020-00386-1
  30. Gilbert PM, Hofmann S, Ng HH, Vankelecom H, Wells JM. Organoids in endocrine and metabolic research: current and emerging applications. *Nat Rev Endocrinol*. 2024;20(4):195-201.  
doi: 10.1038/s41574-023-00933-1
  31. Wang J, Zhou D, Li R, *et al*. Protocol for engineering bone organoids from mesenchymal stem cells. *Bioact Mater*. 2025;45:388-400.  
doi: 10.1016/j.bioactmat.2024.11.017
  32. Zhao D, Saiding Q, Li Y, Tang Y, Cui W. Bone Organoids: Recent Advances and Future Challenges. *Adv Healthc Mater*. 2023;13(5).  
doi: 10.1002/adhm.202302088
  33. Cai Y, Xiong M, Xin Z, *et al*. Decoding aging-dependent regenerative decline across tissues at single-cell resolution. *Cell Stem Cell*. 2023;30(12):1674-1691.e8.  
doi: 10.1016/j.stem.2023.09.014
  34. Wang D, Villenave R, Stokar-Regenscheit N, Clevers H. Human organoids as 3D in vitro platforms for drug discovery: opportunities and challenges. *Nat Rev Drug Discov*. 2025;25(3):204-226.  
doi: 10.1038/s41573-025-01317-y
  35. Wang J, Zhang H, Qu Y, *et al*. An eighteen-organ microphysiological system coupling a vascular network and excretion system for drug discovery. *Microsyst Nanoeng*. 2025;11(1).  
doi: 10.1038/s41378-025-00933-3
  36. Xue C, Chen L, Wang N, Chen H, Xu W, Xi Z, Sun Q, Kang R, Xie L, Liu X. Stimuli-responsive hydrogels for bone tissue engineering. *Biomater Transl*. 2024;5(3):257-273.  
doi: 10.12336/biomatertransl.2024.03.004